Fabrication and Magnetic investigations of highly uniform CoNiGa alloy Nanowires

Article *in* Journal of Magnetism and Magnetic Materials · February 2017

DOI: 10.1016/j.jmmm.2017.01.074

7 authors, including:

U. Khan
Chinese Academy of Sciences
38 PUBLICATIONS **65** CITATIONS
SEE PROFILE

Muhammad Irfan
Chinese Academy of Sciences
25 PUBLICATIONS **69** CITATIONS
SEE PROFILE

Khalid Javed
Forman Christian College
22 PUBLICATIONS **43** CITATIONS
SEE PROFILE

Journal of Magnetism and Magnetic Materials 432 (2017) 124–128

Contents lists available at ScienceDirect

Journal of Magnetism and Magnetic Materials

journal homepage: www.elsevier.com/locate/jmmm

Fabrication and magnetic investigations of highly uniform CoNiGa alloy nanowires

Wen-Jing Li [a], U. Khan [a], Muhammad Irfan [a], K. Javed [b], P. Liu [a,c], S.L. Ban [c], X.F. Han [a,*]

[a] Beijing National Laboratory for Condensed Matter Physics, Institute of Physics, University of Chinese Academy of Sciences, Chinese Academy of Sciences, Beijing 100190, China
[b] Department of Physics, Forman Christian College, Lahore 5400, Pakistan
[c] School of Physical Science and Technology, Inner Mongolia University, Hohhot 010021, China

ARTICLE INFO

Article history:
Received 21 November 2016
Received in revised form 22 December 2016
Accepted 26 January 2017
Available online 1 February 2017

Keywords:
Electrodeposition
CoNiGa alloy nanowires
AAO templates
Thermal activation effect

ABSTRACT

CoNiGa ternary alloy nanowire arrays were successfully fabricated by simple DC electrodeposition into the anodized aluminum oxide (AAO) templates. A systematic study of the potential and components of the electrolyte were conducted to obtain different components of CoNiGa nanowires. The largest Ga content in the prepared alloy nanowires was about 17%, while for Co and Ni contents which can be controlled in a wide range by adjusting the composition and pH value of the electrolyte appropriately. X-ray diffraction analysis confirmed that the as-grown CoNiGa nanowire arrays were polycrystal with fcc phase of Co where Co atoms partially substituted by Ni and Ga. Magnetization curves of samples with different composition were measured at room temperature as well as low temperature. The results showed that the components of the alloy nanowires have a great impact on its magnetic properties. For $Co_{55}Ni_{28}Ga_{17}$ nanowires, the magnetization reversal mode changes from curling mode to coherent rotation as the angle increases, and the temperature dependence of coercivity can be well described by the thermal activation effect.

1. Introduction

In the recent few decades, magnetic nanostructures have received considerable attention not only for fundamental physical interest but also technological applications such as high density perpendicular magnetic recording medium [1,2], sensors [3], drug delivery [4,5] and various giant magneto- resistance devices [6–8]. Specially, magnetic multi-alloy nanowires have been intensively investigated for its tunable magnetism with variation in elemental proportions. Many techniques have been used to fabricate magnetic nanowires or nanotubes, among them template-assisted electro-chemical deposition is one of the most universal way to make high aspect ratio nanowires with controlled morphology in large area [9–15].

Heusler alloy CoNiGa is known as a promising magnetic shape-memory alloy for higher Curie temperature, better ductility, and excellent superelasticity in comparison with NiMnGa, which is partially hindered by its low martensitic transformation temperature and bad ductility in the polycrystalline state, and also the low blocking stress level [16,17]. So far, lots of efforts have been made to synthesize and explore the microstructures and magnetic properties of CoNiGa alloy in bulk or thin films [18–20]. However, to the best of our knowledge, no research about one-dimensional structures of CoNiGa alloy has been reported yet. In this work, CoNiGa alloy nanowires with different compositions have been fabricated in anodized aluminum oxide (AAO) templates with chemical electrodeposition route. The main challenge of depositing CoNiGa alloy nanowires is the reduction of Ga ion from the electrolyte, as the reduction potential of Ga is much different from that of Co and Ni. By optimizing deposition potential, composition and pH value of electrolyte, we have controlled Ga contents in present system to 17%. Later on, morphology and magnetic properties of CoNiGa nanowires embedded in AAO templates were investigated as a function of elemental composition.

2. Experiment methods

To fabricate CoNiGa nanowires, AAO templates with an average diameter of 200 nm were used. Prior to electrodeposition, Cu seed layer with thickness of 200 nm was sputtered on one side of AAO template to serve as a conducting electrode. A conventional three electrode cell was used potentiostatically at room temperature with a platinum foil and saturated calomel electrode (SCE-KCl) worked as counter and reference electrodes, respectively. Different deposition potential was applied from −1.1 V to −1.6 V

* Corresponding author.
E-mail address: xfhan@iphy.ac.cn (X.F. Han).

http://dx.doi.org/10.1016/j.jmmm.2017.01.074
0304-8853/

(vs. SCE) in a fixed solution composed of 26 g L^{-1} $CoSO_4{\cdot}7H_2O$, 20 g L^{-1} $NiSO_4{\cdot}6H_2O$, 34 g L^{-1} $Ga_2(SO_4)_3{\cdot}18H_2O$ and 20 g L^{-1} $C_6H_5Na_3O_7{\cdot}2H_2O$ to obtain best reduction potential for Ga ions, since it is much more difficult to deposit compared with Co and Ni. Then, nanowires with different compositions were controlled with modified electrolytic solution and the optimized potential.

Morphological and structural characterizations were performed with field emission scanning electron microscope (FE-SEM: Hitachi S-4800) and X-ray diffraction (XRD: RIGAKU-D/MAX-2400), respectively. Chemical composition of nanowires was determined by Energy-Dispersive X-ray analysis (EDX) attached with FE-SEM. Room temperature and low temperature magnetic measurements were done by vibrating sample magnetometer (VSM: Microsense EV-9) and Physical Property Measurement System (PPMS: Quantum Design-9T), respectively.

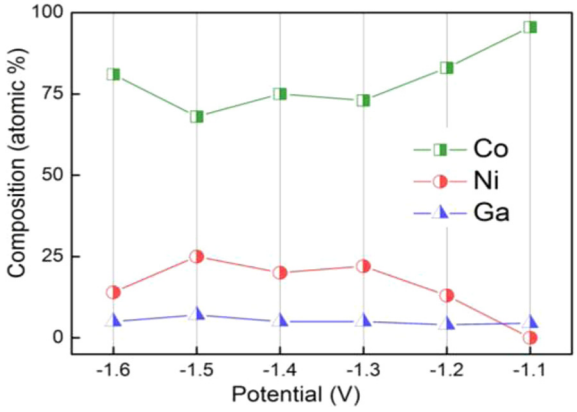

Fig. 1. Compositions of Co, Ni, and Ga in as-deposited nanowires varied with the deposition potential.

3. Results and discussion

The variation of Co, Ni and Ga composition against potential is represented in Fig. 1. It is clear that for both Ga and Ni reduction the most favorable potential is −1.5 V and under this potential nanowires with excellent morphology can be acquired. Thus, in the subsequent experiments we fixed the deposition potential at −1.5 V and carefully optimized deposition parameters to get different ratio of alloy nanowires.

Fig. 2a, b and c show the SEM images of the prepared $Co_{75}Ni_{20}Ga_5$, $Co_{54}Ni_{34}Ga_{12}$ and $Co_{55}Ni_{28}Ga_{17}$ alloy nanowires after removing the AAO templates, respectively. The inset in Fig. 2a represents the morphology of $Co_{75}Ni_{20}Ga_5$ nanowire arrays at low magnification, which depicts large density, clean, homogeneous and aligned nanowires. Morphology predicts that prepared nanowires have diameter of 200±20 nm, similar to the pore size of AAO templates. During deposition, we found that nanowire alloy with Ga contents less than 17% exhibit excellent morphology and for above that they become partially broken, which can be attributed to the formation of $Ga(OH)_3$ while increasing the amount of gallium sulfate in the solution during electrodeposition. This eventually restricts the improvement of Ga contents in nanowires. In other case, For Co and Ni contents, which can be controlled easily with variation in nickel and cobalt sulfate in prepared electrolyte. It is worth mentioning that the pH of electrolyte also has strong impact on the reduction of Co and Ni. Fig. 2d is a typical EDX spectrum for $Co_{55}Ni_{28}Ga_{17}$. The extra peaks in EDX spectrum (C and O) are present due to the cleaning procedure with ethanol, water and etchant, whereas, Al peak is attributed to the partial etching of AAO template with NaOH, and Au is introduced for better conductivity during the SEM process.

Fig. 3 is the XRD spectrum for $Co_{55}Ni_{28}Ga_{17}$ and $Co_{57}Ni_{36}Ga_7$ nanowires in as-deposited state. The XRD was performed at room temperature and analysis indicates that the three main peaks at about 44.2°, 51.5°, and 75.7° are corresponding to face centered

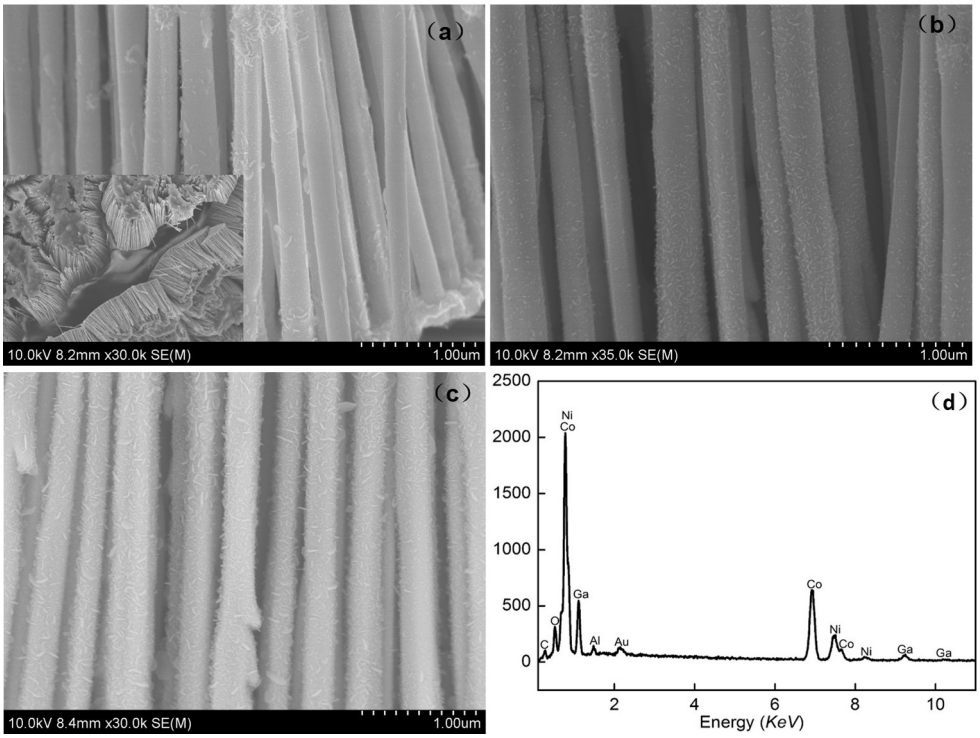

Fig. 2. SEM images of (a) $Co_{75}Ni_{20}Ga_5$, (b) $Co_{54}Ni_{34}Ga_{12}$, and (c) $Co_{55}Ni_{28}Ga_{17}$ nanowires after removing the AAO templates, (d) energy dispersive X-ray (EDX) spectrum of $Co_{55}Ni_{28}Ga_{17}$ nanowires.

cubic (fcc) phase of Co with Bragg's peaks (111), (200) and (220), respectively. It is well reported in literature that for pure Co, hcp-crystal phase is more stable than fcc structure at room temperature. But as Ni is largely incorporated in the Co crystal structure, the hcp phase disappears and fcc-crystal phase was detected. A similar results have already been confirmed by previous study [21,22]. The average crystallite size of $Co_{55}Ni_{28}Ga_{17}$ and $Co_{57}Ni_{36}Ga_7$ are about 13 nm and 25 nm, respectively, calculations using Scherrer equation.

The room temperature magnetization curves of CoNiGa samples at different compositions measured with magnetic field parallel and perpendicular to the axis of nanowires are shown in Fig. 4. The corresponding coercive fields *Hc* and remanence ratio *Mr/Ms* derived from the magnetization curves are listed in Table 1. As observed, the remanence ratio *Mr/Ms* are quite close in parallel and perpendicular directions for all samples, indicating that the alloy nanowires have no obvious easy axis. We attribute this behavior to the balance of two major factors: one is the shape anisotropy owing to the large aspect ratio of nanowires, favoring a longitudinal easy axis; another is the magnetostatic interactions among nanowires, which prefer a transverse easy axis [23]. As the distance between two neighboring nanowires is about 300 nm according to SEM image, not much larger than the diameter of nanowires, thus the magnetostatic interactions between nanowires is remarkable. In addition, from XRD analysis we conclude that the as-grown nanowires are polycrystalline structure without significant preferred orientation, thus in the above discussion we have ignored the contribution of magnetocrystalline anisotropy [24]. The coercivity *Hc* exhibits a strong dependence on the composition of the nanowires, with 37% enhancement in parallel direction from 110 Oe to 151 Oe, and the magnetization decreases slightly when increasing the Ga content. Thus, it is feasible to tailor the magnetic properties of the nanowires by varying the ratio of the elements.

To explore the magnetization reversal behavior of the as-deposited CoNiGa alloy nanowires, we measured the hysteresis loops of $Co_{55}Ni_{28}Ga_{17}$ in different directions from 0° to 90° with respect to the axis of the nanowires at room temperature. As shown in Fig. 5b, with the increase of angle, the coercivity first increases, reaching its maximum value at 30°, then decrease gradually. Usually, there are two main mechanisms to describe the magnetization reversal process of the magnetic nanostructures: coherent rotation and curling mode. In coherent rotation mode, coercivity decreases with angle, while curling mode gives an opposite behavior [25,26]. Therefore, in our case for small angles ($\theta \leqslant 30°$) the magnetization reversal occurs mainly via curling model, but for larger angles ($\theta > 30°$) the coherent rotation is dominant. It is worth mention that the threshold diameter between

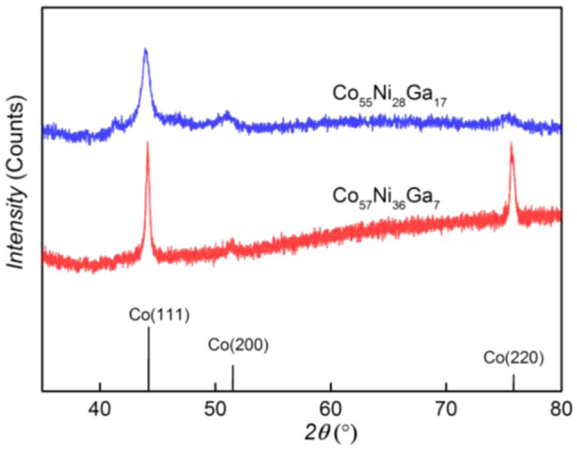

Fig. 3. XRD pattern of $Co_{55}Ni_{28}Ga_{17}$ and $Co_{57}Ni_{36}Ga_7$ nanowires.

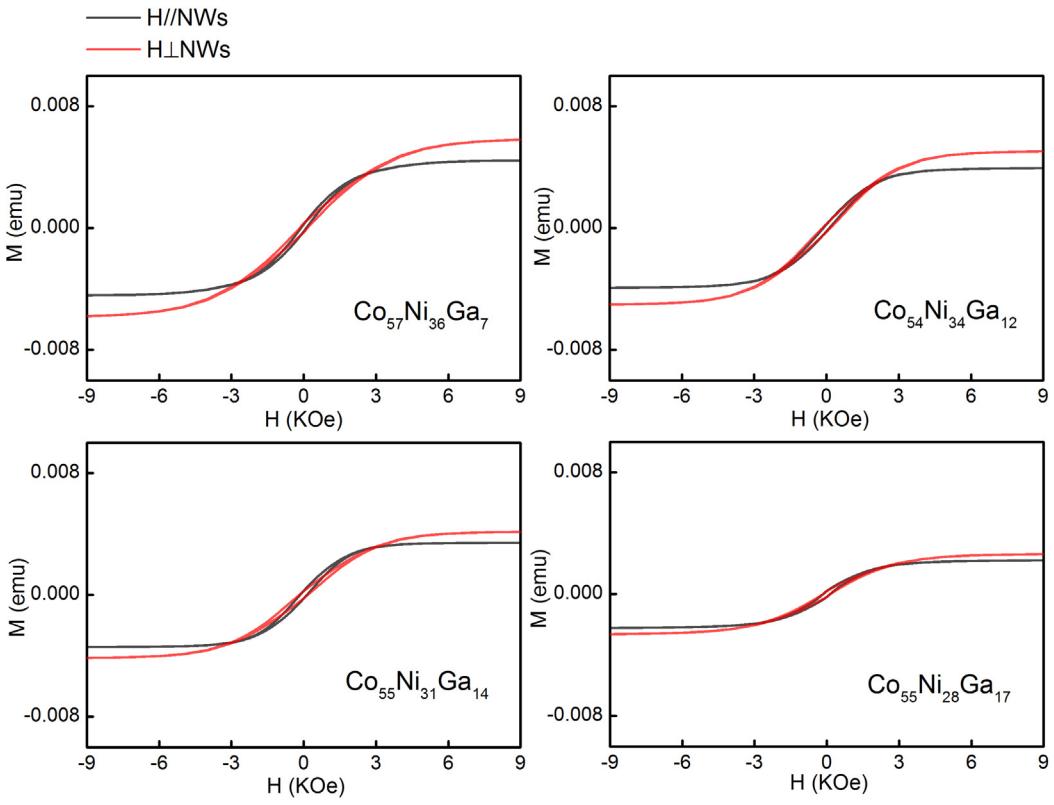

Fig. 4. Magnetization curves of CoNiGa samples at different compositions in parallel and perpendicular directions.

Table 1
Magnetic parameters: coercivity *Hc* and remanence ratio *SQ* in parallel and perpendicular directions of four CoNiGa samples.

Samples	$Hc_{//}$ (Oe)	$SQ_{//}$ (*Mr/Ms*)	$Hc_{\perp}$ (Oe)	$SQ_{\perp}$ (*Mr/Ms*)
$Co_{57}Ni_{36}Ga_7$	110	0.05	154	0.05
$Co_{54}Ni_{34}Ga_{12}$	125	0.06	166	0.05
$Co_{55}Ni_{31}Ga_{14}$	140	0.07	173	0.06
$Co_{55}Ni_{28}Ga_{17}$	151	0.09	144	0.08

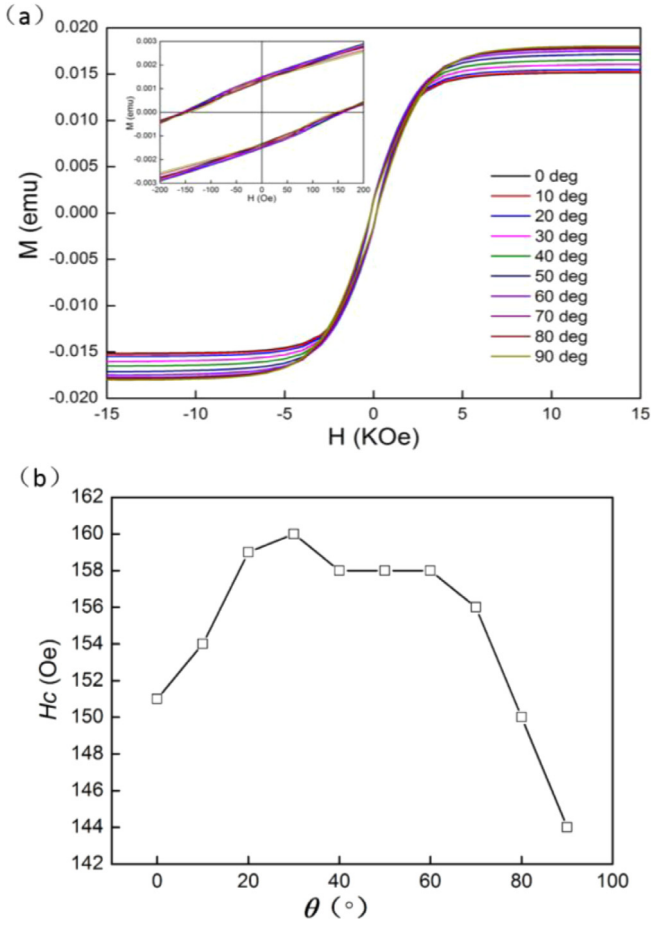

Fig. 5. Hysteresis loops of $Co_{55}Ni_{28}Ga_{17}$ sample from 0° to 90° and its angular dependence of coercivity *Hc*.

coherent rotation and curling is d_c, and for wire diameter $d \ll d_c$, the reversal occurs by coherent rotation. For wire diameter $d > d_c$, the reversal occurs by curling or maybe domain wall motion. When wire diameter d approaches d_c, the curling mode appears at small θ, while coherent rotation arises at larger θ [27], as the situation in our experiment. This result indicates that the d_c of our as-prepared nanowires are comparable to 200 nm. However, considering that for nanowire arrays without magnetostatic interactions, the d_c will be much smaller than 200 nm. Thus we believe that the magnetostatic interactions does exist in our samples as discussed previously and results in the significant enhancement of d_c [25].

Fig. 6 illustrates the temperature dependence of coercivity with the field applied parallel to the nanowire axis for $Co_{55}Ni_{28}Ga_{17}$ sample measured by PPMS. The deviation of the data is 5% due to the measurement principle of PPMS, marked with the error bars. It is demonstrated that the coercivity increases almost linearly with decreasing temperature from 400 K to 5 K. As the temperature decrease further, the increment in coercivity becomes faster, indicating a strong temperature dependent characteristic. To interpret this behavior, we also investigated the variation of saturation magnetization with temperature, not shown here. The result manifests that the saturation magnetization merely reduces 7% when raising the temperature from 5 K to 400 K, which is insufficient to lead to such a decrease in *Hc*. Therefore, we attribute the main reason for the rapid decline of coercivity to the thermal activation effect during the magnetization reversal process. Here, we consider thermal effect over the energy barrier proposed by Neel and Brown, the coercivity can be described by [28–31]

$$H_C(T) = H_0\left\{1 - \left[\frac{K_B T \ln(f_0\tau)}{KV}\right]^{\frac{1}{m}}\right\},$$

where H_0 is the switching field without thermal fluctuation, and KV is the anisotropy energy. f_0 and τ are the attempt frequency and relaxation time, respectively. Based on the above formula, we found that when $m = 1$ the fitting curve can match the experimental data quite well, as indicated in the red dotted line in Fig. 6. In general,

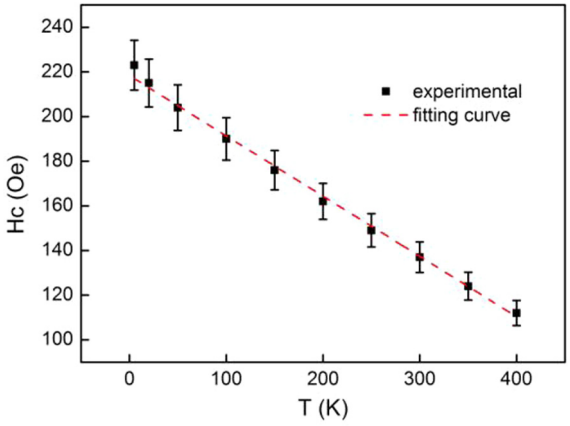

Fig. 6. Temperature dependence of coercivity *Hc* for $Co_{55}Ni_{28}Ga_{17}$.

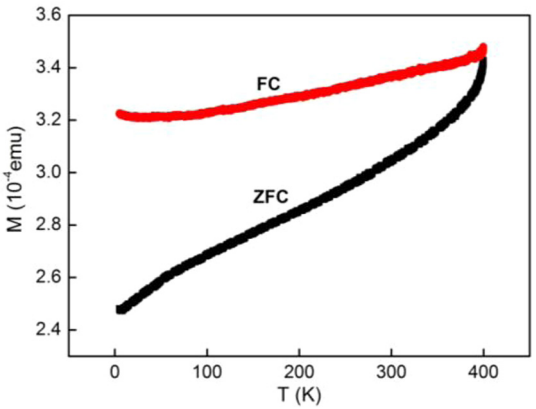

Fig. 7. ZFC and FC magnetic moments measurements carried out in 50 Oe field.

$m = 2$ is corresponding to aligned Stoner-Wohlfarth particles without interaction, and $m = 3/2$ reflects a nonsymmetric energy landscape [29]. Previously, there is also some reports on the linear dependence of coercivity on temperature [32], but the explanation for such a behavior is still lacking. Fig. 7 shows the temperature dependence of magnetic moments in field-cooled (FC) and zero-field-cooled (ZFC) modes with applied field of 50 Oe for $Co_{55}Ni_{28}Ga_{17}$ samples. It is known that CoNiGa alloy with the stoichiometry close to Co_2NiGa usually exhibits abrupt change in magnetization when going through the martensitic and magnetic phase transitions. From Fig. 7, we found that our sample shows ferromagnetic behavior from 5 K to 400 K without phase transition.

4. Conclusion

In this article, we have successfully fabricated different composition of CoNiGa alloy nanowires by DC electrodeposition. XRD pattern revealed that the as-deposited CoNiGa alloy are polycrystalline structure. The magnetic properties of four CoNiGa samples with varied component were investigated at room temperature, and the angular dependence of coercivity curve for $Co_{55}Ni_{28}Ga_{17}$ confirmed that the magnetostatic interactions plays an important role in the magnetization reversal process. Low temperature magnetic studies indicated that the coercivity of the nanowires decreases rapidly with increasing temperature, following the thermal activation model.

Acknowledgments

This work was supported by the State Key Project of Fundamental Research and 863 Plan Project of Ministry of Science and Technology [MOST 2014AA032904]; the MOST National Key Scientific Instrument and Equipment Development Projects [Grant No. 2011YQ120053]; the National Natural Science Foundation of China [NSFC, Grant No. 11374351 and 11434014]; the Strategic Priority Research Program (B) of the Chinese Academy of Sciences (CAS) [Grant No. XDB07030200], and the user fund of Wuhan National High Magnetic Field Center [PHMFF2015011].

References

[1] M. Albrecht, A. Moser, C.T. Rettner, S. Anders, T. Thomson, B.D. Terris, Writing of high-density patterned perpendicular media with a conventional longitudinal recording head, Appl. Phys. Lett. 80 (2002) 3409–3411.
[2] M. Albrecht, C.T. Rettner, A. Moser, M.E. Best, B.D. Terris, Recording performance of high-density patterned perpendicular magnetic media, Appl. Phys. Lett. 81 (2002) 2875–2877.
[3] L. Kang, D. He, L. Bie, P. Jiang, Nanoporous cobalt oxide nanowires for non-enzymati electrochemical glucose detection, Sens. Actuators, B 220 (2015) 888–894.
[4] H. Wu, G. Liu, X. Wang, J. Zhang, Y. Chen, J. Shi, H. Yang, H. Hu, S. Yang, Solvothermal synthesis of cobalt ferrite nanoparticles loaded on multiwalled carbon nanotubes for magnetic resonance imaging and drug delivery, Acta Biomater. 7 (2011) 3496–3504.
[5] S.J. Son, J. Reichel, B. He, M. Schuchman, S.B. Lee, Magnetic nanotubes for magnetic-field-assisted bioseparation, biointeraction, and drug delivery, J. Am. Chem. Soc. 127 (2005) 7316–7317.
[6] L. Piraux, K. Renard, R. Guillemet, S. Mátéfi-Tempfli, M. Mátéfi-Tempfli, V.A. Antohe, S. Fusil, K. Bouzehouane, V. Cros, Template-grown NiFe/Cu/NiFe nanowires for spin transfer devices, Nano Lett. 7 (2007) 2563–2567.
[7] R. Mattheis, S. Glathe, M. Diegel, U. Hübner, Concepts and steps for the realization of a new domain wall based giant magnetoresistance nanowire device: From the available 24 multiturn counter to a 212 turn counter, J. Appl. Phys. 111 (2012) 113920.
[8] P. Shakya, B. Cox, D. Davis, Giant Magnetoresistance and Coercivity of electrodeposited multilayered FeCoNi/Cu and CrFeCoNi/Cu, J. Magn. Magn. Mater. 324 (2012) 453–459.
[9] F. Li, L. Song, D. Zhou, T. Wang, Y. Wang, H. Wang, Fabrication and magnetic properties of $NiFe_2O_4$ nanocrystalline nanotubes, J. Mater. Sci. 42 (2007) 7214–7219.
[10] I.A. Banerjee, L. Yu, M. Shima, T. Yoshino, H. Takeyama, T. Matsunaga, H. Matsui, Magnetic nanotube fabrication by using bacterial magnetic nanocrystals, Adv. Mater. 17 (2005) 1128–1131.
[11] F. Chen, F. Wang, F. Jia, J. Li, K. Liu, S. Huang, Z. Luan, D. Wu, Y. Chen, J. Zhu, R.-W. Peng, M. Wang, Periodic magnetic domains in single-crystalline cobalt filament arrays, Phys. Rev. B 93 (2016) 054405.
[12] Y. Zhang, M. Liu, B. Peng, Z. Zhou, X. Chen, S.-M. Yang, Z.-D. Jiang, J. Zhang, W. Ren, Z.-G. Ye, Controlled phase and tunable magnetism in ordered iron oxide nanotube arrays prepared by atomic layer deposition, Sci. Rep. 6 (2016) 18401.
[13] J. Chen, Y. Wang, Y. Deng, Highly ordered $CoFe_2O_4$ nanowires array prepared via a modified sol–gel templated approach and its optical and magnetic properties, J. Alloys Comp. 552 (2013) 65–69.
[14] A. Pérez-Junquera, J.I. Martín, M. Vélez, J.M. Alameda, J.L. Vicent, Temperature dependence of the magnetization reversal process in patterned Ni nanowires, Nanotechnology 14 (2003) 294–298.
[15] A. Kawahito, T. Yanase, T. Endo, T. Nagahama, T. Shimada, Fabrication of Fe nanowires on yittrium-stabilized zirconia single crystal substrates by thermal CVD methods, J. Appl. Phys. 117 (2015) 17D506.
[16] M. Siewert, M.E. Gruner, A. Dannenberg, A. Hucht, S.M. Shapiro, G. Xu, D.L. Schlagel, T.A. Lograsso, P. Entel, Electronic structure and lattice dynamics of the magnetic shape-memory alloy Co_2NiGa, Phys. Rev. B 82 (2010) 064420.
[17] A. Talapatra, R. Arróyave, P. Entel, I. Valencia-Jaime, A.H. Romero, Stability analysis of the martensitic phase transformation in Co_2NiGa Heusler alloy, Phys. Rev. B 92 (2015) 054107.
[18] Y. Kishi, C. Craciunescu, M. Sato, T. Okazaki, Y. Furuya, M. Wuttig, Microstructures and magnetic properties of rapidly solidified CoNiGa ferromagnetic shape memory alloys, J. Magn. Magn. Mater. 262 (2003) L186–L191.
[19] J. Liu, H. Xie, Y. Huo, H. Zheng, J. Li, Microstructure evolution in CoNiGa shape memory alloys, J. Alloys Comp. 420 (2006) 145–157.
[20] E. Dogan, I. Karaman, Y.I. Chumlyakov, Z.P. Luo, Microstructure and martensitic transformation characteristics of CoNiGa high temperature shape memory alloys, Acta Mater. 59 (2011) 1168–1183.
[21] V. Vega, T. Böhnert, S. Martens, M. Waleczek, J.M. Montero-Moreno, D. Görlitz, V.M. Prida, K. Nielsch, Tuning the magnetic anisotropy of Co–Ni nanowires: Comparison between single nanowires and nanowire arrays in hard-anodic aluminum oxide membranes, Nanotechnology 23 (2012) 465709.
[22] M. Vázquez, L.G. Vivas, Magnetization reversal in Co-base nanowire arrays, Phys. Status Solidi B 248 (2011) 2368–2381.
[23] A. Encinas-Oropesa, M. Demand, L. Piraux, I. Huynen, U. Ebels, Dipolar interactions in arrays of nickel nanowires studied by ferromagnetic resonance, Phys. Rev. B 63 (2001) 104415.
[24] M. Zheng, R. Skomski, Y. Liu, D.J. Sellmyer, Magnetic hysteresis of Ni nanowires, J. Phys. Condens. Matter 12 (2000) L497–L503.
[25] G.C. Han, B.Y. Zong, P. Luo, Y.H. Wu, Angular dependence of the coercivity and remanence of ferromagnetic nanowire arrays, J. Appl. Phys. 93 (2003) 9202–9207.
[26] S. Shamaila, D.P. Liu, R. Sharif, J.Y. Chen, H.R. Liu, X.F. Han, Electrochemical fabrication and magnetization properties of CoCrPt nanowires and nanotubes, Appl. Phys. Lett. 94 (2009) 203101.
[27] W.F. Brown, Criterion for uniform micromagnetization, Phys. Rev. 105 (1957) 1479–1482.
[28] J.-H. Gao, Q.-F. Zhan, W. He, D.-L. Sun, Z.-H. Cheng, Synthesis and magnetic properties of Fe_3Pt nanowire arrays fabricated by electrodeposition, Appl. Phys. Lett. 86 (2005) 232506.
[29] H. Zeng, R. Skomski, L. Menon, Y. Liu, S. Bandyopadhyay, D.J. Sellmyer, Structure and magnetic properties of ferromagnetic nanowires in self-assembled arrays, Phys. Rev. B 65 (2002) 134426.
[30] X.Y. Zhang, G.H. Wen, Y.F. Chan, R.K. Zheng, X.X. Zhang, N. Wang, Fabrication and magnetic properties of ultrathin Fe nanowire arrays, Appl. Phys. Lett. 83 (2003) 3341–3343.
[31] D.J. Sellmyer, M. Zheng, R. Skomski, Magnetism of Fe, Co and Ni nanowires in self-assembled arrays, J. Phys.: Condens. Matter 13 (2001) R433–R460.
[32] N. Grobert, W.K. Hsu, Y.Q. Zhu, J.P. Hare, H.W. Kroto, D.R.M. Walton, M. Terrones, H. Terrones, Ph. Redlich, M. Rühle, R. Escudero, F. Morales, Enhanced magnetic coercivities in Fe nanowires, Appl. Phys. Lett. 75 (1999) 3363–3365.